Investigations of freezing behavior of refrigerants for applications below −80°C

Katharina STÖCKEL[1]*, Robert LOW[2], Yixia XU[1], Christiane THOMAS[1]

[1]Technische Universität Dresden, Schaufler Chair of Refrigeration, Cryogenics and Compressor Technology,
Dresden, Germany
kaharina.stoeckel@tu-dresden.de

[2] Orbia Fluor & Energy Materials, Thornton Science Park, Pool Lane, Ince,
Chester, England

* Corresponding Author

ABSTRACT

For demanding ultra-low-temperature applications such as environmental test chambers, refrigeration systems must operate reliably at temperatures of −80 °C and below. The selection of a suitable refrigerant is therefore not only constrained by its thermodynamic performance and environmental properties, but also critical regarding its behavior close to the solidification limit. While the freezing point is an important benchmark, the actual freezing process - including the behavior during subcooling, the crystallization dynamics, and the partial solidification - can significantly influence the operational stability of the system and so the applicability of a refrigerant below its nominal freezing temperature. In this work, the freezing behavior of several newly designed zeotropic refrigerant mixtures is investigated and compared with the commercially available refrigerant R-473A. The mixtures examined consist of R-744 (carbon dioxide), R-1132a (trifluoromethyl ethylene), R-125 (pentafluoroethane), R-116 (hexafluoroethane), R-23 (trifluoromethane), and R-32 (difluoromethane) in various combination and compositions. The aim is to identify refrigerant mixture that achieve freezing points below −80 °C, keeping in mind a low Global Warming Potential (GWP) for this field of application. The experimental analyses are supported by thermodynamic modelling. The experimental analysis focused on determining the beginning of freezing, the solidification range, and the potential of sub-freezing operation. The results show that some of the investigated zeotropic mixtures exhibit partial solidification without complete phase separation. Compared to R-473A, selected mixtures achieved comparable or lower freezing points down to −94 °C.

1. INTRODUCTION

The Regulation (EU) No. 2024/573 (Union, 2024) on fluorinated gaes (F-gas regulation) entered into force in 2024 and strengthens the EU's F-gas framework aiming to reduce the emissions of fluorinated greenhouse gases (F-gases) by 95 % by 2030. To achieve this goal, it is essential to develop and implement new refrigeration technologies that use alternative refrigerants with low global warming potential (GWP). Hydrofluorocarbons (HFCs) including those used in refrigeration application for temperatures below −50°C, fall within the reinforced phase-down until a phase-out is reached and restriction measures. Although specific exception remains for ultra-low temperature (ULT) [1] application, the industry is in need for alternative refrigerants that have a low GWP without compromising system performance, safety or reliability. Currently, R-23 - despite its extremely high GWP of approximately 14,800 (IPCC, 2023)- is still widely used in ULT applications due to its favorable thermodynamic properties, including a normal boiling point of −82°C and non-flammability.

[1] Ultra-low temperature refers to a temperature range between −50 °C and −100 °C (ASHRAE, 2002)

Refrigerant options for ULT applications include natural substances such as carbon dioxide (R-744), ethylene (R-1150), and ethane (R-170) as well as synthetic refrigerants such as R-32 and R-1132a, as well as their mixtures. In recent years, zeotropic blends such as R-469A, R-472A, R-472B, and R-473A have gained significant attention. All of these blends reach temperatures down to −70 °C and are not flammable. A theoretical study by Giménez-Prades et al. demonstrated that in a two-stage cascade refrigeration system achieving a minimum temperature of −70°C, R-473A attained the highest Coefficient of Performance (COP) among the evaluated blends – R-469A, R-472A, and R-472B – indicating superior thermodynamic efficiency (Giménez-Prades, Udroiu, Navarro-Esbrí, & Mota-Babiloni, 2025). To verify the theoretical investigation Giménez-Prades used R-469A and R-472B as drop-in refrigerants for a two-stage cascade refrigeration system. Both refrigerant mixtures successfully passed the pull-down test down to −70°C with a reduction of the energy consumption of up to 17 % at −50 °C compared to R23 (Giménez-Prades, Navarro-Esbrí, Udroiu, Barragán-Cervera, & Mota-Babiloni, 2026). According to Winkler et al. (Winkler, Cop, Barta, & Hesse, 2022) R-473A is another option to substitute R-23 in environmental test chambers with high temperature stability.

Despite these advancements, there remains a need for refrigerants capable of operating reliably below −80°C. Additionally, further reduction of the GWP compared to R-23 is desirable to support long-term environmental sustainability. In this context, zeotropic mixtures composed of natural and synthetic refrigerants offer a promising pathway. By leveraging differences in volatility and phase behavior, these mixtures can be tailored to achieve lower freezing points than the existing blends. In this study, a series of newly designed zeotropic mixtures based on R-744, R-1132a, R-125, R-116, R-23, and R-32 are investigated, exploring their potential to operate reliably below −80°C. Since some blends still contain a certain amount of R-23, this results in a higher GWP of the blend, while others mixtures, with e.g., R-1132a, offer a better environmental profile but may necessitate modifications to the safety architecture of the refrigeration system. To balance these trade-offs, an experimental analysis was conducted to investigate the freezing behavior of some new mixtures, focusing on the onset of freezing, solidification range, and subcooling behavior, supported by a thermodynamic modelling of the solid–liquid equilibrium.

2. THEORETICAL CALCULATION

A theoretical thermodynamic model was set up to estimate the vapor-liquid-solid equilibria (VLSE) for multicomponent mixtures of R-744 with one or more fluorocarbon refrigerants. This was based on the Schröder equation (Schröder, 1986) for the correlation between solubility and the activity of R-744 dissolved in the liquid phase and was further extended to account for the fugacity of each individual substance in the vapor phase:

$$\ln(\gamma_j x_j) = -\frac{\Delta H_{fus,j}}{RT}\left[1 - \frac{T}{T_{fus}}\right] \tag{1}$$

The equation (1) describes the solubility of a solid in the liquid phase (SLE) depending on temperature T, linking the activity coefficient (γ_j), mole fraction (x_j), enthalpy of fusion ($\Delta H_{fus,j}$), melting temperature (T_{fus}) and universal gas constant R.

$$f_i^V = \phi_i^v P_T y_i = f_{i,s}^* = \gamma_i p_i^* \phi_i^* x_i \tag{2}$$

Equation (2) describes the phase equilibrium (VLSE) by equating the fugacities of each component in the vapor (f_i^V), liquid, and solid phases ($f_{i,s}^*$) using pure component vapor pressure (p_i^*), mole fraction in the liquid phase x_i and mole fraction in the vapor phase y_i. To account for non-idealities, it incorporates fugacity coefficients (ϕ) and activity coefficients (γ). The fugacity of pure solid R-744 was estimated from known literature data (de Guido, Langè, Moioli, & Pellegrini, 2014).

Vapor-liquid equilibrium (VLE) data were regressed for each binary refrigerant mixture using the Redlich-Kwong equation for the vapor-phase fugacity coefficients (Redlich-Kwong, 1949) and the Wilson equation (Wilson, 1964) with temperature-dependent interaction parameters for the liquid-phase activity coefficients. If no literature data were available or if the measurements were not performed at temperatures near the triple point of pure R-744, the VLE of selected pairs was studied in-house using an equilibrium cell apparatus capable of operating to −65°C. This meant that the activity coefficients were extrapolated from the range of measured VLE data to the expected freezing point range only over a limited temperature range of 10-20 K.

The selected samples are: pure R-473A (GWP of 1830), sample 1 R-744/R-1132a/R-32, sample 2 R-744/R-1132a/R-23/R-125 and sample 3 R-744/-R-1132a/R-23/R-116/R-125. Calculated with a GWP of 1 for R-744 (A1), 771 for R32 (A2L), 14600 for R-23 (A1), 3740 for R-125 (A1), 0.052 for R-1132a (A2) and 12400 for R116 (A1) according to IPCC AR6 (IPCC, 2023). The GWP reduction compared to R-23 is for R-473A 87 %, for sample 1 99 %, for sample 2 77 % and for sample 3 75 %. All refrigerant mixtures but sample 3 with R-116 are free of PFAS (per- and polyfluoroalkyl substances). With regard to the composition, it can be assumed that sample 1 will be classified as flammable, while the other mixtures will most likely be classified as midly flammable. A final classification still needs to be carried out.

Table 1: Selected and investigated refrigerant mixtures with theoretical freezing point

Sample ID	Composition	Theoretical freezing point (°C)	Bubble point pressure (kPa)	GWP
0	R-473A [R-744/R-1132a/R-23/R-125 60/20/10/10 wt. %]	−69.8	256	1830
1	R-744/R-1132a/R-32 (40/40/20 wt. %)	−87.6	82	155
2	R-744/R-1132a/R-23/R-125 (38/26/18/18 wt. %)	−85.4	93	3338
3	R-744/R-1132a/R-23/R-116/R-125 (34/28/12/18/18 wt. %)	−85.2	116	3685

The VLSE model was further used to estimate the variation of temperature with vapor quality in the three-phase region at two pressures that were anticipated to cause dry ice formation in part of the region. The predictions of the model for the R-473A composition are compared with those calculated from REFPROP (Lemmon, Bell, Huber, & McLinden, 2018) using Span-Wagner equation of state for the fluid in Figure 1. The REFPROP model predictions are shown as dashed lines. They deviate by 1-2 K from the VLSE model with the deviation increasing at lower pressures.

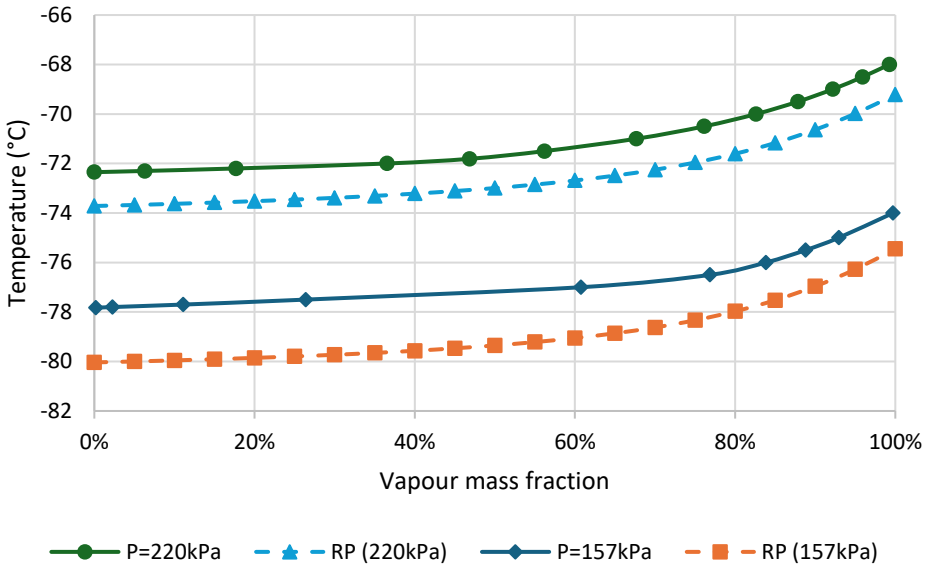


Figure 1: Temperature change during vaporization of R-473A at different constant pressures comparing REFPROP (RP) in dashed lines with the VLSE model in solid lines.

3. METHODOLOGY

3.1 Measurement Principles

In this paper the freezing point is detected using the method of Rossini, which use a geometrical analysis of the freezing and melting curve of a fluid (Mair, Augustus, & Rossini, 1941) (Streiff & Rossini, 1944). Both the freezing range and the melting point can be used to determine the solidification of the liquid. According to Mair (Mair, Augustus, & Rossini, 1941) a metastable liquid can be detected if the cooling rate is low enough, resulting in a clearly visible subcooling in the temperature curve (see Figure 2). The subcooling of the liquid takes place between points A and C, as no freezing nuclei forms, thus enabling subcooling below the actual solidification point. The temperature increases from point C to point D can be explained with the phase change from the metastable state to the three-phase equilibrium (solid, liquid and gaseous) according to Pfennig (Pfennig, 2013). The liquid solidifies and an equilibrium between the three phases is established. The fluid then continues to cool (D to E). In the analysis, the slope of the subsequent cooling is extended until the tangent intersects the cooling curve – see Figure 2 point A. The area enclosed between the temperature curve and the tangent is divided into two equal areas – shown in yellow and blue in Figure 2. The point where the bisector intersects the tangent line is the freezing point – point B.

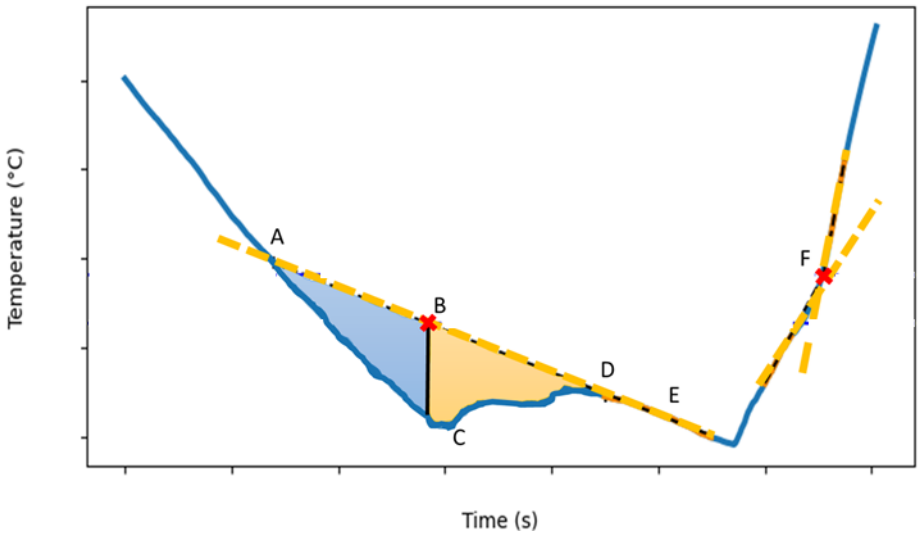


Figure 2: Schematic calculation method for freezing and melting point according to Rossini

When using a constant heating supply, the melting point of the fluid is characterised by a change in the temperature gradient. In the evaluation, a tangent is applied to the temperature curve after the constant heat supply has started and a tangent after the fluid has completely liquefied. The intersection of the two tangents is the melting point (point F) – see Figure 2. The average of the melting point and the freezing point is called the solidification point in this paper.

3.2 Measurement Set-Up

The refrigerant (mixture) under test is filled into a glass measuring cell capable of withstanding pressures up to 1 MPa and is housed in a double-walled, temperature-controlled vessel. The temperature is controlled using a Julabo FP91-Sl thermostat with ethanol, achieving a minimal temperature of approximately −87 °C in the measuring cell. During the measurement the temperature of the thermostat is kept constant. Lower temperatures can be reached using liquid nitrogen, supplied by a Dewar vessel. A schematic of the test setup and a photo of one measuring cell is provided in Figure 3. For heating the measuring cell, a Peltier-element which is located at the bottom of the cell is used. Due to the measuring cell's resistance to negative absolute pressure, filling with the refrigerant (mixture) starts at a temperature below −40 °C, with enough liquid added to ensure that the temperature sensor is in the liquid phase of the sample. A PT100 temperature sensor with an uncertainty of 0.1 K (k=2) and a pressure sensor with a relative uncertainty of 0.025 bar are used. The freezing process can be observed through a sight glass.

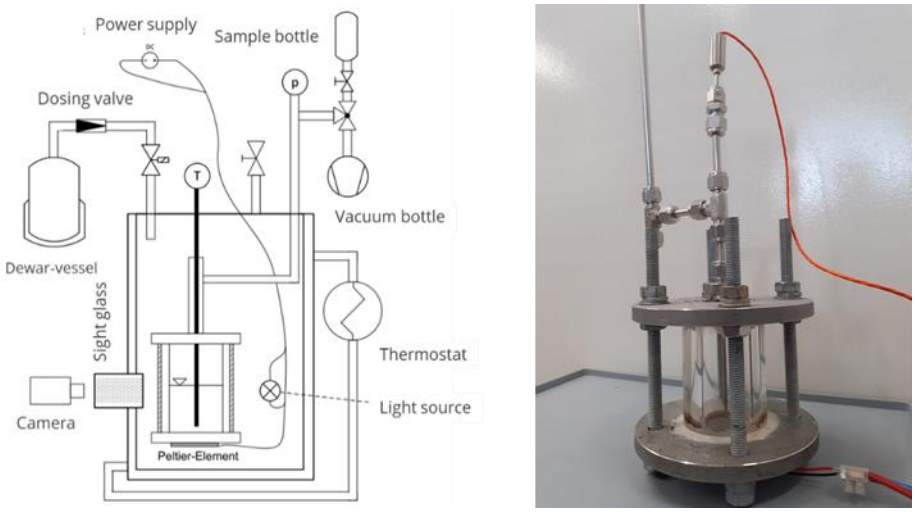


Figure 3: Schematic (Göpfert & Hesse, 2018) and photo of freezing point measurement test cell.

The data collected during the freezing point test is recorded in real time and must be analysed graphically to determine the final values for both the melting point and the freezing point of the refrigerant being tested.

4. EXPERIMENTAL RESULTS

For all samples the freezing point as well as the melting point are measured and the average freezing temperature and melting temperature are calculated. In Table 1 the theoretical freezing point and the composition of the sample are listed. The freezing point of R-473A, measured over eight runs, is used as the baseline value.

As an example, the temperature curve of the third test run of the measurement of R-473A is shown in Figure 4. In this run a metastable area between 5700 s and 6200 s can be detected. Using the tangent of the linearly decreasing temperature, the freezing point is located at −70.7 °C. The intersection of the two tangents at the melting point occurs at approximately 6750 s at −70.2 °C. All measurements were analyzed in this manner.

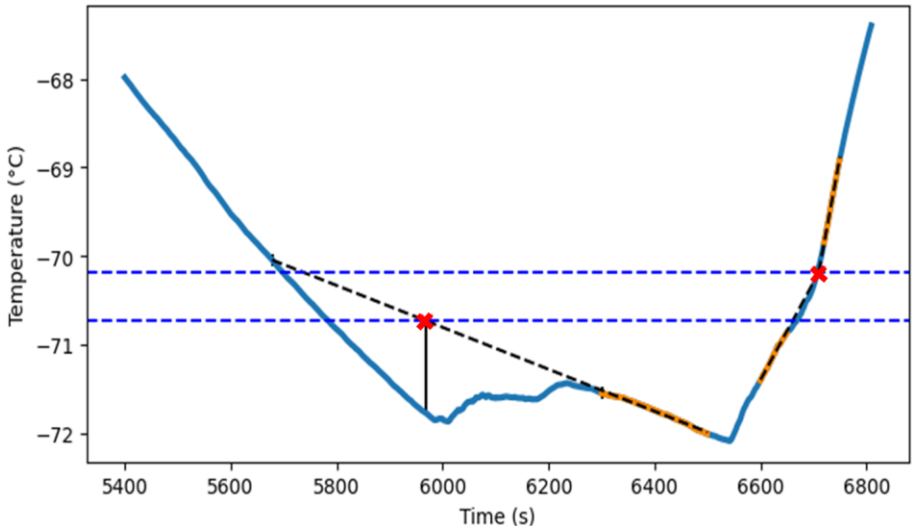


Figure 4: Measured temperature curve of R-473A

In Figure 5 the freezing point and melting point of each tested refrigerant (mixture) is shown and leads to an average freezing point of −71.9 °C and an average melting point of −71.2 °C, which leads to an average temperature of −71.54 °C. Compared with the theoretical freezing point of −69.8 °C the measured is 1.8 K respectively 3 % lower.

The measurement for sample 1 with R-744/R-1132a/R-32 (40/40/20 wt. %) reached the minimum temperature of the measuring cell of -86.1 °C without solidification. To investigate the freezing point liquid nitrogen is used for cooling the measuring cell down. In Figure 5 the temperature curve for the freezing as well as for the melting point is shown. In this case the freezing point at −94 °C indicates the beginning of the freezing, and the “melting point” the end of the solidification at −130 °C. In this context, the so-called "melting point" refers to the temperature at which liquefaction begins when heated. This suggests that a liquid-gas-solid phase exists over a temperature range of approximately 36 K, from −94 °C to −130 °C. However, an accurate freezing point for sample 1 could not be determined, because no subcooled liquid was detected, likely due to the increased cooling rate with the liquid nitrogen. Compared with R-473A, the freezing point is lower and reaches the target value of −80 °C; compared to the estimated temperature from the theoretical model, the actual temperature is 6.5 K, respectively 7 % lower.

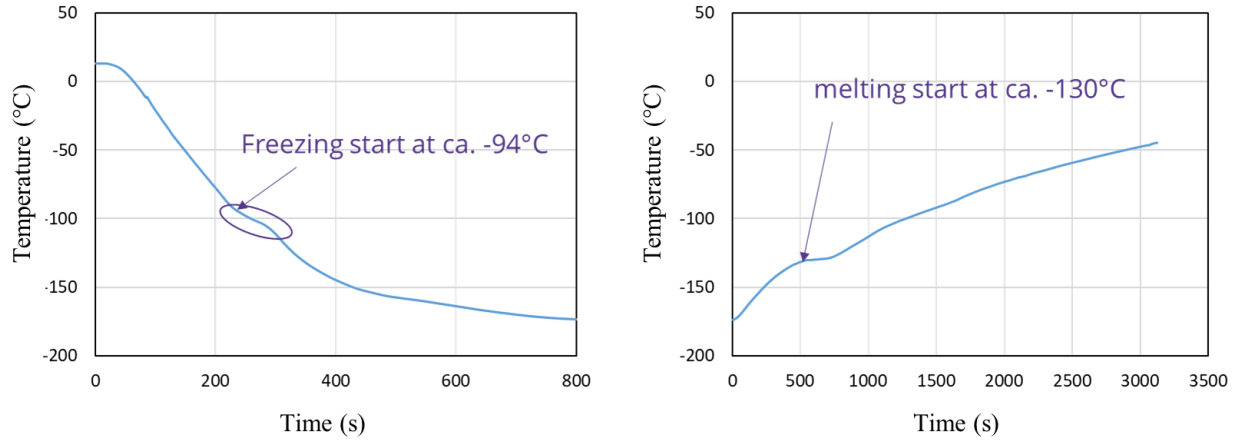


Figure 5: Temperature curve of sample 1. left: cooling down with freezing point. right: heating up with melting point.

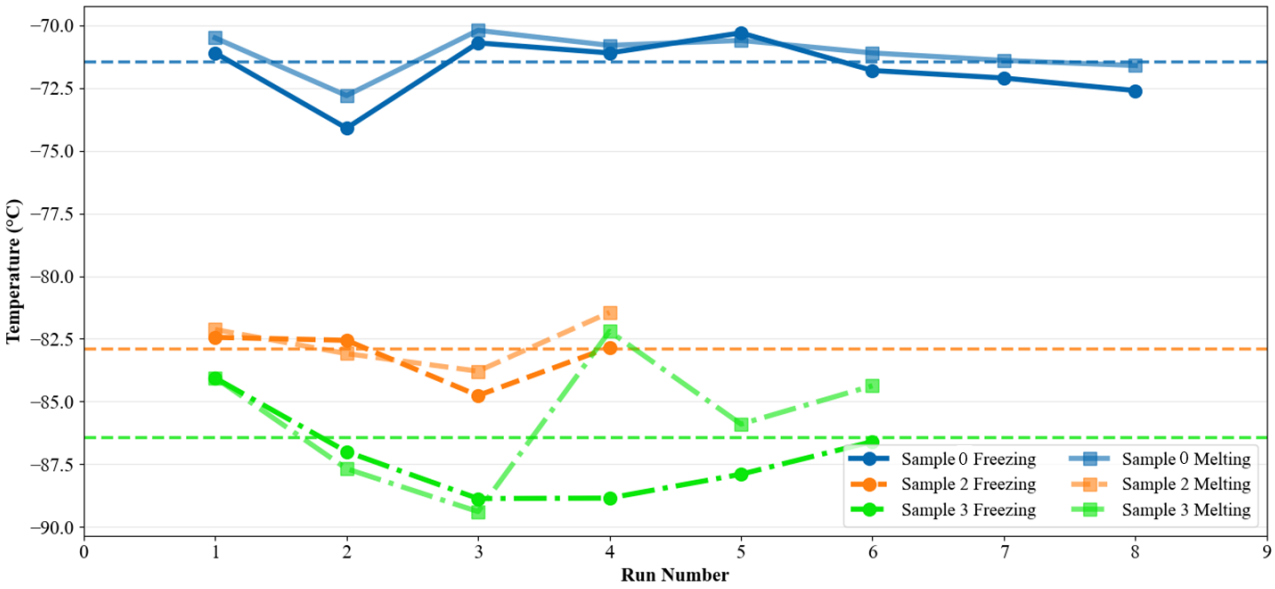


Figure 6: Freezing and melting point temperature of all samples with average temperature

For the four-componant sample 2 with R-744/R-1132a/R-23/R-125 (38/26/18/18 wt. %) the freezing point was estimated to be −85.4 °C. Similar to the measurement of R-473A the freezing point and melting point were identified. Figure 6 shows the measured freezing and melting points for each measurement, with the average freezing point at −83.8 °C and the average melting point at −82.5 °C. The determined mean solidification point is −82.9 °C, thus also meeting the target of −80 °C. Compared to the calculated freezing point, the deviation is 3 % and the achieved temperature is 2.5 K higher. Figure 7 shows a picture of the vapor-liquid-solid-equilibrium at approximately −84.5 °C.



Figure 7: Solidification state of sample 2 at -84.5 °C at point E (Figure 2)

Sample 3 with five components R-744/R-1132a/R-23/R-116/R-125 (34/28/12/8/18 wt. %) also achieved a freezing point below −80 °C with a freezing temperature of −86.3 °C as can be seen in Figure 7. In Figure 8 photos of the different freezing stages, referred to point C, D and E in Figure 2 are shown. At point A the freezing at the surface area started at the end of the metastable area. The solid parts settle to the bottom, and the solidification process continues, as can be seen at point D. At point D, solidification advances and the bottom is covered with solids. A liquid phase exists above the solids, and crystals form at the interface between the liquid and the gas. It should be noted that this is a vapor-liquid-solid equilibrium and that complete solidification has not yet been achieved. Compared to the estimation freezing point of −86.3 °C, the reached temperature is 1.2 K lower with a relative deviation is 1 %.

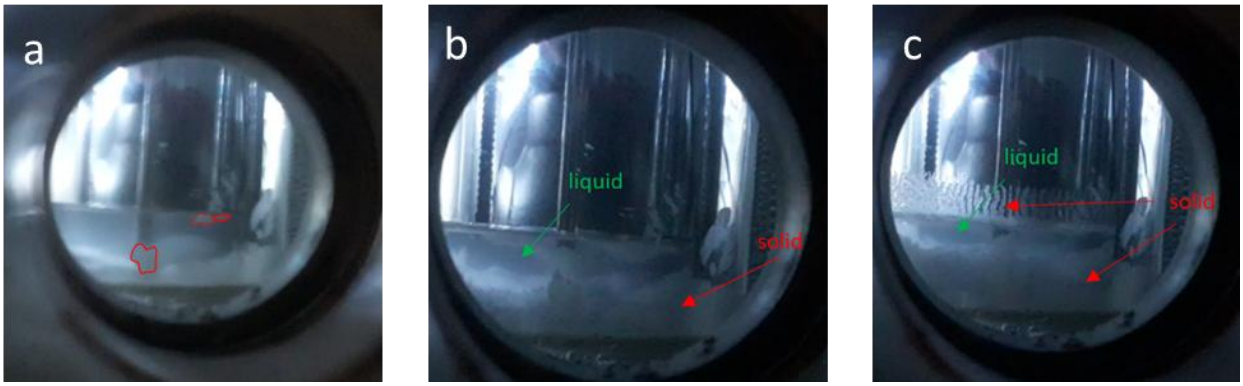


Figure 8: Sample 3 at three different temperature points. a) at point C with first solid particles highlighted in red. b) at point D with increasing solid fraction c) at point E solidification on liquid-gas-surface

6. CONCLUSIONS

The solidification of four different zeotropic refrigerant mixtures was investigated to achieve a temperature below -80 °C. As the baseline, R-473A with a freezing temperature of −71.5 °C was used. For selecting the composition of the investigated refrigerant mixture, an approach of calculating the theoretical freezing point based on Schröder was presented. Compared with R-23 a reduction of the GWP between 75 % and 99 % could be achieved.

All three alternative refrigerant mixtures achieved a solidification point below −80 °C, and thus can be used in ULT application. However, it is important to note that the pressure of the normal boiling point can be below ambient pressure, meaning that some mixtures technically cannot be operated at −85 °C without significant challenges regarding the component selection. Sample 1 with the three components R-744, R-1132a and R-32 (40, 40 and 20 wt. %) has an estimated solidification point of −87.6 °C and a measured one of −94 °C. Thus, the relative deviation between theoretical and experimental result is 7 %. The second refrigerant mixture has four components: R-744, R-1132a, R-32, and R-125 (38, 26, 18 and 18 wt. %) and an estimated solidification temperature of −85.4°C. The experimental solidification temperature is −82.9 °C with a derivation of 3% to the theoretical temperature. The third refrigerant mixture with five components - R-744, R-1132a, R-23, R-116, and R-125 (34, 28, 12, 18 and 18 wt. %) has a theoretical solidification temperature of −85.2 °C. Compared with the experimental solidification temperature of −86.6 °C the derivation is 1%. Within the next investigations, a system test will be carried out to check the limits of the substances during the operation of a ULT cycle, particularly with regard to blocking depending on the operating point. Also, the new approach for the theoretical calculation of the solidification temperature for mixtures with R-744 shows a good comparability with the measured values and will be used for further developments.

NOMENCLATURE

f	fugacity	(kPa)
H	enthalpy	(J/mol)
P	pressure	(kPa)
R	gas constant 8.31447	(J/mol/K)
T	temperature	(K)
x	liquid mole fraction	(-)
y	vapor mole fraction	(-)
ϕ	fugacity coefficient	(-)
γ	activity coefficient	(-)

Subscript/Superscript

fus	fusion as in heat of fusion
j	component ‘j’ (solute) in multicomponent mixture
l	liquid phase
s	solid phase
tot	total pressure
v	vapor phase
*	pure component

REFERENCES

ASHRAE. (2002). 2002 ASHRAE handbook: Refrigeration (I-P ed.). (R. a.-C. Society of Heating, Ed.)

de Guido, G., Langè, S., Moioli, S., & Pellegrini, L. (2014). Thermodynamic method for the prediction of solid CO2 formation from multicomponent mixtures. *Process Safety and Environmental Protection*, *92*(1), 70-79.

Giménez-Prades, P., Navarro-Esbrí, J., Udroiu, C. M., Barragán-Cervera, Á., & Mota-Babiloni, A. (2026). Experimental evaluation of low-GWP refrigerants as drop-in alternatives to R23 for ultra-low temperature refrigeration. *Thermal Science and Engineering Progress*.

Giménez-Prades, P., Udroiu, C. M., Navarro-Esbrí, J., & Mota-Babiloni, A. (2025). Thermodynamic Evaluation of Low-GWP A1 Refrigerants for Ultra-Low Temperature Refrigeration Applications. *Energies*.

Göpfert, T., & Hesse, U. (2018). Fest-Flüssig-Gleichgewichte des ternären Stoffgemisches Kohlenstoffdioxid-Ethan-Ethylen. *DKV-Jahrestagung*.

IPCC, C. W. (2023). Climate Change 2023: Synthesis Report. Contribution of Working Groups I, II and III to the Sixth Assessment Report of the Intergovernmental Panel on Climate Change. doi:10.59327/IPCC/AR6-9789291691647

Lemmon, E. W., Bell, I. H., Huber, M. L., & McLinden, M. O. (2018). NIST Standard Reference Database 23: reference Fluid Thermodynamic and Transport Properties-REFPROP ,Version 10.0. (N. I. Technology, Ed.)

Mair, B. J., Augustus, R., & Rossini, F. D. (1941). Determination of freezing points and amounts of impurity in hydrocarbons from freezing and melting curves. *Journal of Research of the National*.

Pfennig, A. (2013). Thermodynamik der Gemische. (Springer-Verlag, Ed.)

Redlich-Kwong. (1949). On the thermodynamics of solutions. V. An equation of state. Fugacities of gaseous solutions. *Chem. Rev., 44*, pp. 233-244.

Schröder, M. (1986). Beitrag zur Bestimmung thermophysikalischer Eigenschaften von mischungen synthetischer Kältemaschinenöle mit Ein- und Zweistoffkältemitteln. Forschungsberichte des Deutschen Kälte- und Klimatechnischen Vereins.

Streiff, A., & Rossini, F. (1944). Method for Determining Individual Hydrocarbons in Mixtures of Hydrocarbins by Measurement of Freezing Points. *U.S. Department of Commerce, Reasearch Paper RP1584, Journal of Research of National Bureau of Standards, 32*.

Union, O. J. (2024). Regulation (EU) 2024/573 of the European Parliament and of the Council of 7 February 2024 on fluorinated greenhouse gases, amending Directive (EU) 2019/1937 and repealing Regulation (EU) No 517/2014 (Text with EEA relevance) .

Wilson, G. M. (1964). Vapor-liquid equilibrium. XI. A new expression for the excess free energy of mixing. *Journal of the American Chemical Society*.

Winkler, T., Cop, M., Barta, R. B., & Hesse, U. (2022). Experimental Investigation of a New Ultra-Low Temperature Refrigerant in an Environmental Test Chamber. *19th International Refrigeration and Air Conditioning Conference at Purdue*.